

Noise-like pulse based on dissipative four-wave-mixing with photonic crystal fiber filled by reduced graphene oxide

Lei Gao, Tao Zhu,* and Wei Huang

Key Laboratory of Optoelectronic Technology & Systems (Ministry of Education), Chongqing University, Chongqing 400044, China

*Corresponding author: zhutao@cqu.edu.cn

A noise-like pulse based on dissipative four-wave-mixing in a fiber cavity with photonic crystal fiber filled by reduced graphene oxide is proposed. Due to large evanescent field provided by 3 cm photonic crystal fiber and ultrahigh nonlinearity of reduced graphene oxide, this mixed structure provides excellent saturable absorption and high nonlinearity, which are necessary for generating four-wave-mixing (FWM). We experimentally prove that the mode-locked laser transfers its energy from center wavelength to sidebands through degenerate FWM, and new frequencies are generated via cascaded FWM among those sidebands. During this process, the frequencies located in various orders of longitudinal modes of the ring cavity are supported, and others are suppressed due to destructive interference. As the longitudinal modes of the cavity with a spacing of 6.874 MHz are partially supported, the loosely fixed phase relationship results in noise-like pulse with a coherent peak of 530 fs locating on a pedestal of 730.693 ps. © 2014 Optical Society of America

OCIS Codes: (060.3510) Lasers, fiber, (060.4370) Nonlinear optics, fibers, (190.4380) Nonlinear optics, four-wave mixing

Passively mode-locked fiber laser (ML) has drawn intense interests in both scientific and industrial applications, and the engineering with group velocity dispersion (GVD), loss and gain, filtering, polarization, and nonlinearity makes it functioning in various states, such as conventional soliton, self-similar laser, dissipative soliton, etc [1-4]. Particularly, when the laser operating condition is altered, or more nonlinear processes are involved, a laser cavity can generate a kind of noise-like pulse (NLP) comprising a bunch of pulses with noise-likely varying width and intensity [5-9]. Compared with soliton lasers, NLP possesses a much lower coherence, and its autocorrelation trace contains a coherence peak of femtosecond duration locating on a broad pedestal ranging from several to hundreds of picoseconds [8]. Its optical bandwidth is often comparable to or even larger than the gain bandwidth of active fiber, and its power can be much larger than that of conventional soliton [7-10]. It has been shown that NLP performs better in generating smooth supercontinuum, as no spectral modulation ever shown around the pump wavelength due to its stochastic character [11], and it can also be used for optical coherence tomography, radar, and sensing requiring low coherence [12].

NLP can be found in laser cavity with net normal or anomalous GVD, and its formation involves specific nonlinearity, birefringence, gain, and polarization state. Horowitz et al. attribute the generation of NLP to cavity nonlinear transmission and walk-off between two polarizations [5], and a maximum spectral width requires specific dispersion and birefringence [13,14]. Tang et al. prove that NLP formed in nonlinear polarization rotation (NPR) cavity is originated from the combined effect of soliton collapse and positive cavity feedback [15], and they increase the spectral width of NLP to 120 nm via Raman self-frequency shift and four-wave-mixing (FWM) by a zero GVD fiber [7]. Assisted by 12 m highly nonlinear fiber, Jeong et al. produce NLP with a spectral width of 135 nm due to Raman gain enhancement [16]. Wang et al. demonstrate NLP via inserting single wall carbon nanotubes as saturable absorber (SA) into a ring cavity,

and the oversaturation of SA and excessive nonlinear phase shift may attribute to formation of NLP [17].

Here, we propose a NLP based on dissipative FWM in a fiber cavity with photonic crystal fiber (PCF) filled by reduced graphene oxide (rGO). Conventionally, dissipative FWM has been found in fiber cavity with a high finesse Fabry-Perot interferometer or high Q microresonator, through which light is confined to small volume, and cascaded FWM takes place due to enhanced peak power [18,19]. As the free spectral range (FSR) and finesse of those interferometers are relatively high, their adjacent modes, corresponding to different orders of longitudinal modes, can be fully filled with the newly generated frequencies via cascaded FWM. Therefore, stable and coherent soliton train can be generated due to the well fixed frequency spacing of those modes. However, we experimentally find that when the FSR is slightly larger or even comparable to the frequency spacing, the phase of longitudinal modes supported in a fiber cavity is loosely fixed, leading to the formation of NLP.

The principle of NLP based on cascaded FWM is schematically shown in Fig. 1. Similar to the microresonator with high Kerr coefficient, in a ML ring cavity with high nonlinearity, the laser stability is destabilized via modulation instability, and the energy of its center wavelength is transferred to sidebands [20]. Technically, this is a degenerate FWM process, where both the energy conservation ($2\hbar\omega_0 = \hbar\omega_{mS} + \hbar\omega_{mAS}$, where \hbar is the reduced Planck constant, $m = \pm 1, \pm 2, \dots$) and the phase matching condition are satisfied. As shown in Fig. 1 (a), two photons with frequency of ω_0 are annihilated, and two new photons with Stokes frequency (ω_{mS}) and anti-Stokes frequency (ω_{mAS}) are generated simultaneously. The frequencies spacing is represented as $(|2\pi m/L - 2\gamma P|/\beta_{ave})^{1/2}$ [21], where L is period of dispersion, γ is nonlinearity, P is peak power, and β_{ave} is average net dispersion.

During this process, when the nonlinearity of a ML cavity is sufficient high, for example, via interacting with material possessing ultrahigh nonlinearity or confining strongly light to vary small area, nondegenerate FWM

may occur in two possible ways: process 1 of FWM involving interaction between sidebands with center wavelength (such as $\hbar\omega_{1S} + \hbar\omega_{2AS} = \hbar\omega_0 + \hbar\omega_{1AS}$), and process 2 of FWM involving multiple mixing among sidebands without center wavelength (such as $\hbar\omega_{2S} + \hbar\omega_{2AS} = \hbar\omega_{1S} + \hbar\omega_{1AS}$). Besides, degenerate FWM may occur in those new frequencies. Through the cascaded FWM, the energy of center wavelength dissipates into the newly generated frequencies to a large span [21,22]. During those processes, the frequencies located in various orders of longitudinal modes of the ring cavity are supported, and others are suppressed due to destructive interference. However, as the fineness of the fiber ring cavity is relatively low and its FSR is small, as well as the spacings of frequencies generated from the two process are different, the longitudinal modes of this fiber ring cavity may not be fully supported by the cascaded FWM, of which is shown in Fig.1 (b). This leads to loosely fixed phase relationship among longitudinal modes. As more longitudinal modes can be activated, the single pulse width can be very small, but the loosely fixed phase brings randomly variations of width and intensity. This leads to the formation of NLP.

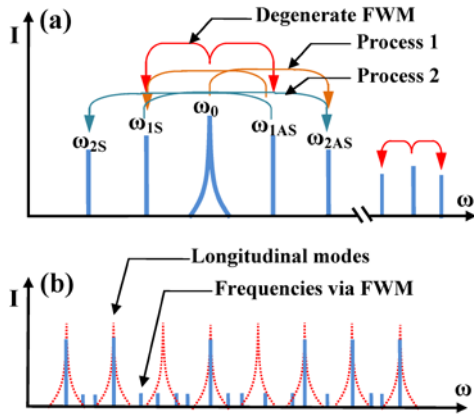


Fig.1 (a), Schematic of FWM in fiber ring cavity, including both degenerate FWM and two possible ways of nondegenerate FWM. (b), The longitudinal modes of the laser cavity are partially supported by new frequencies generated by cascaded FWM.

In this letter, we experimentally demonstrate the NLP operation based on dissipative FWM in a fiber ring cavity with PCF filled by rGO. As a two-dimensional hexagonal packed layer of carbon atoms, graphene exhibits excellent saturable absorption due to the Pauli blocking effect, as well as ultrahigh nonlinearity from π -electron conjugation. [24,25]. Experiments have shown that the nonlinearity of graphene film can be as high as 10^{-6} esu, and it can be further enhanced by long and intense evanescent field interaction, such as fiber taper and PCF [26-30]. FWM based on pristine graphene interacting with fiber taper and photonic crystal nanostructure has been reported, where the effective nonlinearity can be enhanced to 1000 times of that without graphene [31-34]. Recently, a special kind of graphene, rGO that synthesized by oxidation of graphite, has also been found possessing outstanding SA properties and high nonlinearity [28,35-37], and various kinds of MLs based on rGO have been proposed. Previously, we have observed the modulation stability based on 8 mm fiber taper deposited with rGO, and two sidebands are generated [20]. However, a longer fiber

taper is hard to make, and it is fragile and suffered from environmental contamination. So, filling holes of PCF with rGO provides a better solution, and several MLs have been demonstrated [29,36]. In this experiment, we enhance the cavity nonlinearity via filling 3 cm PCF with rGO flakes, and NLP is obtained due to dissipative FWM.

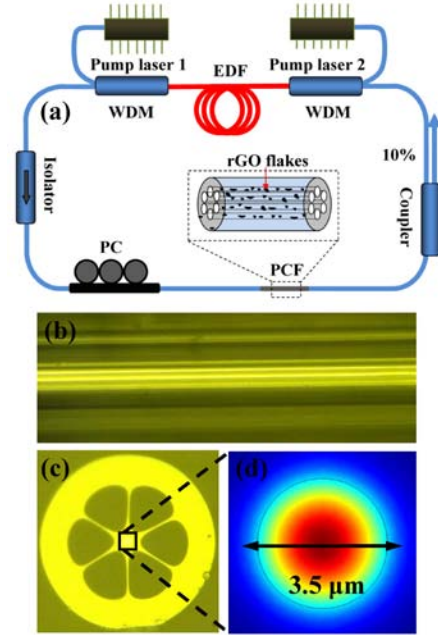


Fig.2 (a), Schematic setup of the fiber ring laser. (b), Photograph of the PCF after rGO deposition. (c) Cross section of PCF and (d) its simulation electric norm distributions of LP₀₁ mode.

The setup of fiber cavity is shown in Fig. 2 (a), incorporating a 1 m erbium-doped fiber (EDF, Liekki ER 80-8/125) with a GVD of 15.7 ps/nm/km that bidirectionally pumped by two 980 nm lasers through two wavelength division multiplexers (WDM), a polarization independent isolator, a polarization controller (PC), an optical coupler with 10% output, 19.5 m dispersion compensation fiber (DCF, DCF38) with dispersion parameter of -38 ps/nm/km, and 8.6 m standard single mode fiber (SMF, Corning SMF-28) with dispersion parameter of 18 ps/nm/km. The net normal dispersion is -0.57 ps/nm, which is necessary to generate NLP. The SA is produced by filling rGO dissolved in N,N-dimethylformamide into the holes of the PCF, which is shown in Fig. 2 (b), and dry in 38° for 24 hours. The parameters of rGO we used and the detail method to make transparent rGO solution is represented in [37], and its size is estimated to be ~ 1 μ m. The cross section of PCF and its stimulated electric norm distributions of LP₀₁ mode are shown in Figs. 2 (c) and (d), respectively. The effective field diameter of 3.5 μ m guarantees both large evanescent field and relative small insertion loss when deposited by rGO flakes. After evaporation, the PCF is spliced between two SMFs, and no interference effect ever been found in the transmission spectrum. The splice loss between pure PCF and SMF is about 3 dB, and the deposition loss of rGO in 3 cm PCF is about 1 dB. The modulation depth of the SA is about 9% detected by a 790 nm laser with a pulse duration of 120 fs. The laser output is monitored by a detector with 3 GHz bandwidth, an

oscilloscope (Lecroy, SDA 8600A), a frequency analyzer (Agilent, PSA E4447A), an autocorrelator (APE, PulseCheck), and an optical spectrum analyzer (Yokogawa, AQ6370).

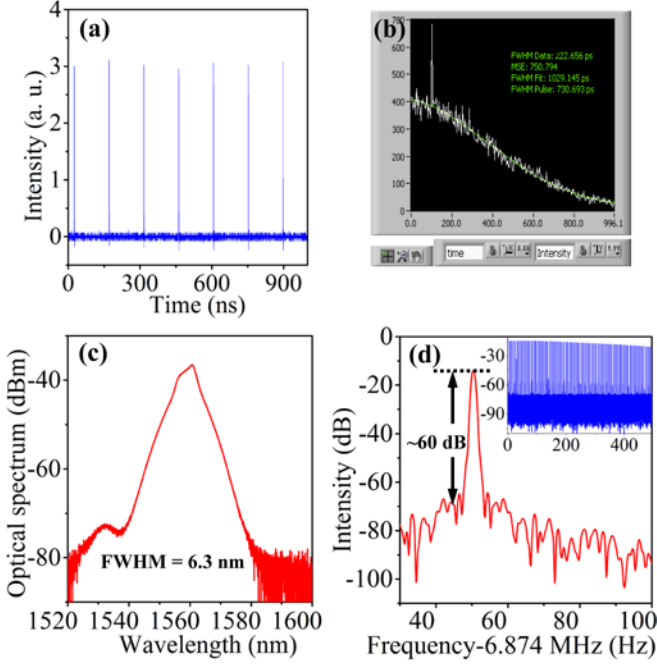


Fig. 3. Characteristics of NLP with two pump lasers both at 200 mW. (a), Pulse train and (b), corresponding autocorrelation trace. (c), optical spectrum with a FWHM of 6.3 nm. (d), Corresponding RF spectra centered at 6.874 MHz, and the inset reveals its RF spectra in a larger range.

After increasing two pump lasers to 200 mW, we rotating PC carefully, and stable NLP can be observed easily. As shown in Fig. 3 (a), the period of pulse train is 145.6 ns, corresponding to a fundamental frequency of 6.874 MHz. As the phases of longitudinal modes are loosely fixed, the intensity fluctuation of the pulse train, defined as $(I_{\max} - I_{\min})/I_{\text{average}}$, is about 5%. Its autocorrelation trace in Fig. 3 (b) shows a pedestal with a full width at half maximum (FWHM) of 730.693 ps, and the coherent spike is about 530 fs. As the pedestal width is comparable to the measuring range of the autocorrelator, a small part of the trace is not shown, but this do not affect the discussion here. The optical spectrum in Fig. 3 (c) posses a FWHM of 6.3 nm, which is smaller than that produced from NPR. The possible reason is that the dissipative FWM is relative weak due to the large insertion loss originating from the splice between PCF with SMF, and also DCF with SMF. The corresponding radio frequency (RF) spectrum in Fig. 3 (d) reveals a contrast ratio of 60 dB near the fundamental frequency, and it is slightly broadened due to the intensity fluctuation. The inset containing RF spectrum to 500 MHz suggests that this NLP has very good stability.

We examine the effects of the SA and the DCF in forming NLP. When the 19.5 m DCF is removed from the cavity, no NLP but only conventional soliton can be found, no matter how the PC's position is adjusted. Besides, the SA is replaced by that produced by depositing a graphene film produced from chemical vapor deposition between two fiber pigtailed as in [27], and also no NLP was found.

Once the SA is removed, neither NLP nor conventional soliton laser could be found. Those experiments indicate that the DCF provide specific dispersion for generating FWM, and the rGO-deposited-PCF is key in offering enough nonlinearity to generate the cascaded FWM.

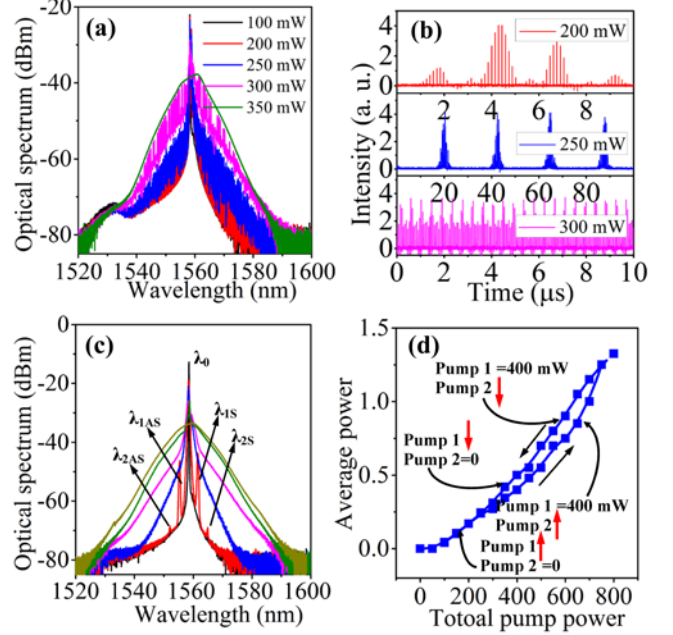


Fig. 4. (a), Optical spectra for different powers of pump 1, and pump 2 is zero. (b), corresponding temporal train detected by oscilloscope. (c), optical spectra under different PC bias, the pump power of the two 980 lasers are both 200 mW. (d), Hysteresis effect of average output power under different pumping routines, arrows indicate the increasing and decreasing of pump laser.

The laser states in different cavity parameters, mainly pump power and polarization state are depicted in Fig. 4. Fig. 4 (a) shows the optical spectra for pump 1 at different values, and pump 2 is zero. It is clearly shown that higher cavity power brings intense FWM, as its optical spectrum is broaden. The corresponding temporal trains in Fig. 4 (b) indicate that a more stable and regular pulse train is formed when increasing pump power, namely from randomly pulse (200 mW) to Q-switched mode-locking (250 mW) and unstable mode-locking (300 mW), suggesting that the NLP was generated through FWM. A careful examination of laser state variation under different polarization states reveals that the laser is destabilized by FWM at first, and then more longitudinal modes are activated through cascaded FWM, finally leading to NLP with broaden optical spectrum. During the experiment, we adjusting the PC slowly, making sure that the polarizations state varies gradually. Although we do not know the actual polarization state of the ring cavity, its relative variation is credible.

The narrowest spectrum shown in Fig. 4 (d) corresponds to a weakly mode-locked laser, which is destabilized when four new frequencies are generated due to degenerate FWM, and its pulse is modulated stochastically. This is consistent to our previous observation based on fiber taper deposited with rGO, which is more detail in [20]. Here, we only focus on the four newly generated wavelengths: $\lambda_{2AS}=1552.108$ nm,

$\lambda_{1AS}=1555.429$ nm, $\lambda_0=1558.43$ nm, $\lambda_{1S}=1561.59$ nm, $\lambda_{2AS}=1565.031$ nm. We find that they both satisfy the energy conservation of the two possible routines of nondegenerate FWM, supporting our explanation about the formation process of NLP. So, it is not surprising to find that frequencies far from center wavelength broaden gradually when changing PC position, as the phase matching condition is optimized. At the same time, the pulse that mode-locked originally by rGO is destabilized due to the energy transfer from center wavelength to newly generated sidebands, and it disappears when the power of center wavelength is comparable to those of the sidebands, and another kind of laser, NLP, is formed.

Hysteresis effect is also observed in this experiment, and the average output powers under different pump routines are shown in Fig. 4 (d). This hysteresis is more obvious when NLP is formed, and its explanation is that the formation of mode-locked, although loosely, longitudinal modes brings relative a higher output power, and the attractive force induced by large net normal GVD intends to keep the mode-locking state even when the pump power goes down [38].

In summary, we proposed a NLP in a fiber cavity with PCF filled by rGO based on dissipative FWM due to the enhanced nonlinearity originating from long evanescent filed interacting length and ultrahigh nonlinearity of rGO. Experimental results demonstrate that the center wavelength of the laser mode-locked purely by rGO dissipates its energy to sidebands through degenerate FWM, and new frequencies are generated via cascaded FWM among those sidebands. As the spacing of the newly generated frequencies is not identical, the longitudinal modes of this fiber ring cavity are not fully supported as in microresonator. This leads to a loosely fixed phase relationship, resulting to NLP with a coherence peak locating on a broad pedestal. Our works provide new information in understanding the dynamics of ML with high nonlinearity, and also find a new way to generate NLP, which may find applications in smooth supercontinuum generation, optical coherence tomography, and sensing.

This work was supported by Natural Science Foundation of China (No. 61377066 and 61405020), and Fundamental Research Funds for Central Universities (No. CDJZR12125502 and 106112013CDJZR120002).

References

1. M. E. Fermann, and I. Hartl, *Nature Photon.* **7**, 868 (2013).
2. X. Liu, D. Han, Z. Sun, C. Zeng, H. Lu, D. Mao, Y. Cui, F. Wang, *Sci. Rep.* **3**, 2718 (2013).
3. K. Kieu, W. H. Renninger, A. Chong, and F. W. Wise, *Opt. Lett.* **34**, 593 (2009).
4. L. Zhao, D. Tang, X. Wu, and H. Zhang, *Opt. Lett.* **35**, 2756 (2010).
5. M. Horowitz, Y. Barad, and Y. Silberberg, *Opt. Lett.* **22**, 799 (1997).
6. L. M. Zhao, D. Y. Tang, J. Wu, X. Q. Fu, and S. C. Wen, *Opt. Express* **15**, 2145 (2007).
7. L. M. Zhao, D. Y. Tang, T. H. Cheng, H. Y. Tam, and C. Lu, *Opt. Commun.* **281**, 157 (2008).
8. Y. Jeong, L. Zuniga, S. Lee, and Y. Kwon, *Opt. Fiber Technol.* <http://dx.doi.org/10.1016/j.yofte.2014.07.004>, (2014).
9. A. Runge, C. Aguergeray, N. Broderick, and M. Erkintalo, *Opt. Lett.* **38**, 4327 (2013).
10. T. North, and M. Rochette, *Opt. Lett.* **38**, 890 (2013).
11. S. Lin, S. Hwang, and J. Liu, *Opt. Express* **22**, 4152 (2014).
12. S. Keren, and M. Horowitz, *Opt. Lett.* **26**, 328 (2001).
13. J. U. Kang, *Opt. Commun.* **182**, 433 (2000).
14. D. Lei, H. Yang, H. Dong, S. Wen, H. Xu, J. Zhang, *J. Mod. Opt.* **56**, 572 (2009).
15. D. Y. Tang, L. M. Zhao, and B. Zhao, *Opt. Express* **13**, 2289 (2005).
16. L. A. Vazquez-Zuniga, Y. Jeong, *Photon. Technol. Lett.* **24**, 1549 (2012).
17. Q. Wang, T. Chen, M. Li, B. Zhang, Y. Lu, and K. P. Chen, *Appl. Phys. Lett.* **103**, 011103 (2013).
18. J. Schröder, T. D. Vo, and B. J. Eggleton, *Opt. Lett.* **34**, 3902 (2009).
19. T. Herr, V. Brasch, J. D. Jost, C. Y. Wang, N. M. Kondratiev, M. L. Gorodetsky, and T. J. Kippenberg, *Nature Photon.* **8**, 145 (2014).
20. L. Gao, T. Zhu, M. Liu, and W. Huang, *arXiv submit/1077089* (2014).
21. N. J. Smith, and N. J. Doran, *Opt. Lett.* **21**, 570 (1996).
22. X. Liu, X. Zhou, C. Lu, *Opt. Lett.* **30**, 2257 (2005).
23. X. M. Liu, *Phys. Rev. A* **77**, 043818 (2008).
24. Z. P. Sun, T. Hasan, F. Torrisi, D. Popa, G. Privitera, F. Q. Wang, F. Bonaccorso, D. M. Basko, and A. C. Ferrari, *ACS. NANO.* **4**, 803 (2010).
25. Q. L. Bao, H. Zhang, Y. Wang, Z. H. Ni, Y. L. Yan, Z. X. Shen, K. P. Loh, and D. Y. Tang, *Adv. Funct. Mater.* **19**, 3077 (2009).
26. E. Hendry, P. J. Hale, J. Moger, and A. K. Savchenko, *Phys. Rev. Lett.* **105**, 097401 (2010).
27. H. Zhang, S. Virally, Q. Bao, L. K. Ping, S. Massar, N. Godbout, and P. Kockaert, *Opt. Lett.* **37**, 1856 (2012).
28. Z. Luo, M. Zhou, D. Wu, C. Ye, J. Weng, J. Dong, H. Xu, Z. Cai, and L. Chen, *Photon. Technol. Lett.* **24**, 1539 (2012).
29. Y. Lin, C. Yang, J. Liou, C. Yu, and G. Lin, *Opt. Express*, **21**, 16763 (2013).
30. Z. Luo, M. Zhou, D. Wu, C. Ye, J. Weng, J. Dong, H. Xu, Z. Cai, and L. Chen, *J. Light. Technol.* **29**, 2732 (2011).
31. B. Xu, A. Martinez, and S. Yamashita, *Photon. Technol. Lett.* **24**, 1792 (2012).
32. T. Gu, N. Petrone, J. F. Mcmillan, A. van der Zande, M. Yu, G. Q. Lo, D. L. Kwong, J. Hone, and C. W. Wong, *Nature Photon.* **6**, 554 (2012).
33. Y. Wu, B. Yao, Y. Cheng, Y. Rao, Y. Gong, X. Zhou, B. Wu, and K. S. Chiang, *Photon. Technol. Lett.* **26**, 249 (2014).
34. A. V. Gorbach, A. Marini, and D. V. Skryabin, *Opt. Lett.* **38**, 5244 (2013).
35. Z. Liu, X. Zhao, X. Zhang, X. Yan, Y. Wu, Y. Chen, and J. Tian, *J. Phys. Chem. Lett.* **2**, 1972 (2011).
36. Z. Liu, X. H, and D. N. Wang, *Opt. Lett.* **36**, 3024 (2011).
37. L. Gao, T. Zhu, W. Huang, J. Zeng, *Appl. Opt.* **53**, 6452 (2014).
38. X. Liu, L. Wang, X. Li, H. Sun, A. Lin, K. Lu, Y. Wang, and W. Zhao, *Opt. Express* **17**, 8506 (2009).

1. M. E. Fermann, and I. Hartl, "Ultrafast fibre lasers," *Nature Photon.* 7, 868-874 (2013).
2. X. Liu, D. Han, Z. Sun, C. Zeng, H. Lu, D. Mao, Y. Cui, F. Wang, "Versatile multi-wavelength ultrafast fiber laser mode-locked by carbon nanotubes," *Scientific reports* 3, 2718 (2013).
3. K. Kieu, W. H. Renninger, A. Chong, and F. W. Wise, "Sub-100 fs pulses at watt-level powers from a dissipative-soliton fiber laser," *Opt. Lett.* 34, 593-595 (2009).
4. L. Zhao, D. Tang, X. Wu, and H. Zhang, "Dissipative soliton generation in Yb-fiber laser with an invisible intracavity bandpass filter," *Opt. Lett.* 35, 2756 (2010).
5. M. Horowitz, Y. Barad, and Y. Silberberg, "Noiselike pulses with a broadband spectrum generated from an erbium-doped fiber laser," *Opt. Lett.* 22, 799-801 (1997).
6. L. M. Zhao, D. Y. Tang, J. Wu, X. Q. Fu, and S. C. Wen, "Noise-like pulse in a gain-guided soliton fiber laser," *Opt. Express* 15, 2145-2150 (2007).
7. L. M. Zhao, D. Y. Tang, T. H. Cheng, H. Y. Tam, and C. Lu, "120 nm bandwidth noise-like pulse generation in an erbium-doped fiber laser," *Opt. Commun.* 281, 157-161 (2008).
8. Y. Jeong, L. A. Vazquez-Zuniga, S. Lee, and Y. Kwon, "On the formation of noise-like pulses in fiber ring cavity configurations," *Opt. Fiber Technol.* <http://dx.doi.org/10.1016/j.yofte.2014.07.004>, (2014).
9. A. Runge, C. Aguerarar, N. Broderick, and M. Erkintalo, "Coherence and shot-to-shot spectral fluctuations in noise-like ultrafast fiber lasers," *Opt. Lett.* 38, 4327-4330 (2013).
10. T. North, and M. Rochette, "Raman-induced noiselike pulses in a highly nonlinear and dispersive all-fiber ring laser," *Opt. Lett.* 38, 890-892 (2013).
11. S. Lin, S. Hwang, and J. Liu, "Supercontinuum generation in highly nonlinear fibers using amplified noise-like optical pulses," *Opt. Express* 22, 4152-4160 (2014).
12. S. Keren, and M. Horowitz, "Interrogation of fiber gratings by use of low-coherence spectral interferometry of noiselike pulses," *Opt. Lett.* 26, 328-330 (2001).
13. J. U. Kang, "Broadband quasi-stationary pulses in mode-locked fiber ring laser," *Opt. Commun.* 182, 433-436 (2000).
14. D. Lei, H. Yang, H. Dong, S. Wen, H. Xu, J. Zhang, "Effect of birefringence on the bandwidth of noise-like pulse in an erbium doped fiber laser," *J. Mod. Opt.* 56, 572-576 (2009).
15. D. Y. Tang, L. M. Zhao, and B. Zhao, "Soliton collapse and bunched noise-like pulse generation in a passively mode-locked fiber ring laser," *Opt. Express* 13, 2289-2294 (2005).
16. L. A. Vazquez-Zuniga, Y. Jeong, "Super-broadband noise-like pulse erbium doped fiber ring laser with a highly nonlinear fiber for Raman gain enhancement," *IEEE Photon. Technol. Lett.* 24, 1549-1551 (2012).
17. Q. Wang, T. Chen, M. Li, B. Zhang, Y. Lu, and K. P. Chen, "All-fiber ultrafast thulium-doped fiber ring laser with dissipative soliton and noise-like output in normal dispersion by single-wall carbon nanotubes," *Appl. Phys. Lett.* **103**, 011103 (2013).
18. J. Schröder, T. D. Vo, and B. J. Eggleton, "Repetition-rate-selective, wavelength-tunable mode-locked laser at up to 640 GHz," *Opt. Lett.* 34, 3902-3904 (2009).
19. T. Herr, V. Brasch, J. D. Jost, C. Y. Wang, N. M. Kondratiev, M. L. Gorodetsky, and T. J. Kippenberg, "Temporal solitons in optical microresonators," *Nature Photon.* 8, 145-152 (2014).
20. L. Gao, T. Zhu, M. Liu, and W. Huang, "Cross-phase modulation instability in mode-locked laser based on reduced graphene oxide," *arXiv submit/1077089* (2014).
21. N. J. Smith, and N. J. Doran, "Modulational instabilities in fibers with periodic dispersion management," *Opt. Lett.* 21, 570-572 (1996).
22. X. Liu, X. Zhou, C. Lu, "Four-wave mixing assisted stability enhancement: theory, experiment, and application," *Opt. Lett.* 30, 2257-2259 (2005).
23. X. M. Liu, "Theory and experiments for multiple four-wave-mixing processes with multifrequency pumps in optical fibers," *Phys. Rev. A* 77, 043818 (2008).
24. Z. P. Sun, T. Hasan, F. Torrisi, D. Popa, G. Privitera, F. Q. Wang, F. Bonaccorso, D. M. Basko, and A. C. Ferrari, "Graphene Mode-locked ultrafast laser," *ACS. NANO.* 4, 803-810 (2010).
25. Q. L. Bao, H. Zhang, Y. Wang, Z. H. Ni, Y. L. Yan, Z. X. Shen, K. P. Loh, and D. Y. Tang, "Atomic-layer graphene as a saturable absorber for ultrafast pulsed lasers," *Adv. Funct. Mater.* 19, 3077-3083 (2009).
26. E. Hendry, P. J. Hale, J. Moger, and A. K. Savchenko, "Coherent Nonlinear Optical Response of Graphene," *Phys. Rev. Lett.* 105, 097401 (2010).
27. H. Zhang, S. Virally, Q. Bao, L. K. Ping, S. Massar, N. Godbout, and P. Kockaert, "Z-scan measurement of the nonlinear refractive index of graphene," *Opt. Lett.* 37, 1856-1858 (2012).
28. Z. Luo, M. Zhou, D. Wu, C. Ye, J. Weng, J. Dong, H. Xu, Z. Cai, and L. Chen, "Graphene-induced nonlinear four-wave-mixing and its application to multiwavelength Q-switched rare-earth-doped fiber lasers," *Photon. Technol. Lett.* 24, 1539-1542 (2012).
29. Y. Lin, C. Yang, J. Liou, C. Yu, and G. Lin, "Using graphene nano-particle embedded in photonic crystal fiber for evanescent wave mode locking of fiber laser," *Opt. Express*, 21, 16763-16776 (2013).
30. Z. Luo, M. Zhou, D. Wu, C. Ye, J. Weng, J. Dong, H. Xu, Z. Cai, and L. Chen, "Graphene-induced nonlinear four-wave-mixing and its application to multiwavelength Q-switched rare-earth-doped fiber lasers," *J. Light. Technol.* 29, 2732-2739 (2011).
31. B. Xu, A. Martinez, and S. Yamashita, "Mechanically exfoliated graphene for four-wave-mixing-based wavelength conversion," *Photon. Technol. Lett.* 24, 1792-1794 (2012).
32. T. Gu, N. Petrone, J. F. Mcmillan, A. van der Zande, M. Yu, G. Q. Lo, D. L. Kwong, J. Hone, and C. W. Wong, "Regenerative oscillation and four-wave mixing in graphene optoelectronics," *Nature Photon.* 6, 554-559 (2012).
33. Y. Wu, B. Yao, Y. Cheng, Y. Rao, Y. Gong, X. Zhou, B. Wu, and K. S. Chiang, "Four-wave mixing in a microfiber attached onto a graphene film," *Photon. Technol. Lett.* 26, 249-252 (2014).
34. A. V. Gorbach, A. Marini, and D. V. Skryabin, "Graphene-clad tapered fiber: effective nonlinearity and propagation losses," *Opt. Lett.* 38, 5244-5247 (2013).
35. Z. Liu, X. Zhao, X. Zhang, X. Yan, Y. Wu, Y. Chen, and J. Tian, "Ultrafast dynamics and nonlinear optical responses from sp²- and sp³-hybridized domains in graphene oxide," *J. Phys. Chem. Lett.* 2, 1972-1977 (2011).
36. Z. Liu, X. H, and D. N. Wang, "Passively mode-locked fiber laser based on a hollow-core photonic crystal fiber filled with few-layered graphene oxide solution," *Opt. Lett.* 36, 3024-3026 (2011).
37. L. Gao, T. Zhu, W. Huang, J. Zeng, "Vector rectangular-shape laser based on reduced graphene oxide interacting with long fiber taper," *Appl. Opt.* 53, 6452-6456 (2014).
38. X. Liu, L. Wang, X. Li, H. Sun, A. Lin, K. Lu, Y. Wang, and W. Zhao, "Multistability evolution and hysteresis phenomena of dissipative solitons in a passively mode-locked fiber laser with large normal cavity dispersion," *Opt. Express* 17, 8506-8512 (2009).